ARCHIVES OF ACOUSTICS
31, 1, 57–76 (2006)

THE SADDLE POINT METHOD APPLIED TO SELECTED PROBLEMS OF ACOUSTICS

A. SNAKOWSKA

University of Rzeszów
Institute of Physics
Rejtana 16a, 35-310 Rzeszów, Poland
e-mail: asnak@univ.rzeszow.pl

H. IDCZAK

Wrocław University of Technology
Institute of Telecommunication and Acoustics
Wybrzeże Wyspiańskiego 27, 50-370 Wrocław, Poland
e-mail: henryk@zakus.ita.pwr.wroc.pl

(*received July 11, 2005; accepted December 9, 2005*)

The paper is aimed at the presentation of examples of applying the saddle point approximation method to some fundamental problems of acoustics and the discussion of some interesting couplings between applied mathematical methods and the physical interpretation of the results.

The saddle point method is shortly reminded in its basic form, from which more advanced versions, improving the results and widening the range of possible applications, are derived. Two problems, solved at first for electromagnetic waves and then applied to acoustics by means of "the analogous method", have been chosen as examples. The first one is the phenomenon of the reflection of a spherical wave at a plane interface between two media, the lower of which is characterised by a higher velocity (water/sand, air/water). In this case there is a critical angle above which a total reflection and a lateral wave occur. The second example is the far field radiated from the outlet of a semi-infinite circular duct. The physical insight into the understanding of the physical phenomena provided by the saddle point method is stressed.

Key words: saddle point method, waves propagation in layered media, lateral wave, radiation from cylindrical duct.

1. Introduction

In the process of the mathematical description of physical phenomena sophisticated mathematical methods as the integral transforms, the integral representation etc., which may darken the physical interpretation of the results, are often applied.

The aim of the paper is to present the saddle point method as a method revealing the physical meaning of the problems considered. We are used to think that the methods of approximate solutions are accepted and applied only because exact solutions are not known. In fact, as will be shown below, in some cases an approximate solution gives more physical insight into the phenomena considered.

Two problems, which have been subjects of our interest for some time, the reflection of sound at a plane interface separating two media and the far field radiated from the semi-infinite cylindrical duct, have been chosen as illustrations of the method. No doubt that they are of considerable theoretical and practical meaning and both were first solved for electromagnetic waves with analogous boundary conditions. The large spectrum of advantages from applying the saddle point method, not only simplifying mathematical formulae but also allowing a clear and meaningful physical interpretation, has been outlined.

Until the forties of the 20-th century, only the problem of reflection of a plane wave at the boundary of two media has been solved analytically. The case often discussed in underwater acoustics, when the sound waves propagate across the boundary with a ratio of velocities $n < 1$ (water/sand, air/water), is analysed below. According to the Snell's law, if the angle of incidence is less than the so-called critical angle, a reflected wave arises together with the transmitted one. For waves incident on the boundary at an angle greater than the critical one, no energy is transmitted to the other medium and the phenomenon of total internal reflection is observed.

It is interesting to consider the case of a plane wave falling on a boundary separating two media at an angle exactly equal to the critical one. Applying the Fermat's principle on extreme propagation time and Huygens principle, one comes to the conclusion that for an angle of incidence equal to the critical one, the incoming wave can propagate over some distance in the lower medium (along the interface) with a greater velocity and come back to the upper medium. In fact, such a wave is observed and called the lateral wave.

Considering propagation in layered media, the application of the ray model requires to take into account all phenomena described above with a reflection coefficient depending on the angle of incidence. The problem has been formulated and solved by BREKHOVSKIKH [1–3] by means of the fundamental paper of WEIL [4] who presented a method of expansion of a spherical wave in the form of an integral over plane waves.

The first attempt to solve the problem of wave propagation in layered media was made by SOMMERFELD for the case of electromagnetic waves [5]. A similar situation occurred in the history of the second problem discussed herein. The problem of radiation from the outlet of a semi-infinite circular duct was originally solved by WAJNSHTEJN for electromagnetic waves [6] and then adapted to sound waves. The results were then generalised for the acoustic field and since then investigated by many authors [7–16].

Section 2 of this paper presents a short description of the saddle point method. Section 3 deals with the representation of a spherical wave in the form of an integral of functions representing plane waves. In Sec. 4, a certain modification of the saddle point method is discussed on the example of the reflection of a spherical wave on the

water/sand interface. It constitutes a fundamental problem in shallow water acoustics. In Sec. 5, the solution for the far field radiated by the outlet of a cylindrical duct serves as an example of another modification of the saddle point method.

2. The saddle point method

The saddle point method [1, 17] is used to calculate approximately contour integrals of the type

$$I(\lambda) = \int_C G(z) e^{\lambda g(z)} \, \mathrm{d}z, \tag{1}$$

where C is the general contour in the complex plane z and λ is a real parameter, $G(z)$ and $g(z)$ are analytic functions of the complex variable z. The background of this method constitutes some properties of the analytic function like: the independence of the integral value of the contour of integration which allows us to deform it as long as no singularities or branch lines are crossed, the Cauchy–Riemann conditions for partial derivatives, the properties of harmonic functions.

Denoting $g(z) = g_R(z) + ig_I(z)$, the exponential function can be written as a product $\exp[\lambda g(z)] = \exp[\lambda g_R(z)] \exp[i\lambda g_I(z)]$, which indicates that the greatest contribution to the integral (1) comes from the vicinity of points in which $g_R(z)$ has its extrema. The real function $g_R(z)$ has its extremum at ξ if both partial derivatives are there equal to zero, $\partial_x g_R(z) = 0$, $\partial_y g_R = 0$. This means, according to Cauchy–Riemann conditions, that the remaining partial derivatives are also equal to zero, $\partial_x g_I(z) = 0$, $\partial_y g_I(z) = 0$. If all four partial derivatives are in a certain point, ξ, equal to zero, the derivative of $g(z)$ is equal to zero at this point: $g'(z) = 0$ for $z = \xi$, where prime indicates differentiation with respect to z. The question arises whether ξ could be a maximum point of $g_R(z)$. Bearing in mind that $g_R(z)$ is a harmonic function and fulfils the equation $\partial_x \partial_x g_R + \partial_y \partial_y g_R = 0$, ξ is a saddle point (Fig. 1) through which at least two curves can be drawn: one has at ξ its maximum, while the other one has there its minimum. Between the family of curves which at the saddle point have their minima or maxima, that one at which the values of the function $g_R(z)$ decrease most rapidly is of our interest. It is called the steepest descend path and likewise is often called the described method. On this curve the phase of the function $\exp[\lambda g(z)]$ is constant.

From what was said above, the main features and basic steps in the saddle point method can be outlined. Moreover, the method is efficient when λ is large and $G(z)$ is a slowly varying function, especially in the neighbourhood of the saddle points, which mostly contribute to the integrand (1).

To recapitulate, the method consists of three main steps:

1. Finding one or more saddle points defined by the criterion $g'(z) = 0$ at $z = \xi$.

2. Respecting all the necessary rules, deform the contour of integration into the steepest descent path, which is defined as the path in the complex plane that passes through the saddle point ξ and along which the real part of $g(z)$ decreases most rapidly.

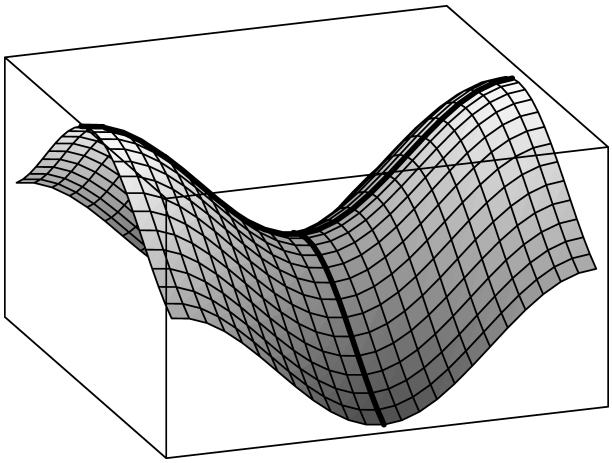

Fig. 1. The steepest descend path and the steepest ascend path crossing the saddle point of an analytic function.

The steepest descent path can be defined by means of a real parameter s

$$g(z) = g(\xi) - s^2 \tag{2}$$

(at every point $z \neq \xi$, $g_R(z) < g_R(\xi)$, what ensures a real s). Equating the last formula with the Taylor series expansion for $g(z)$ about the saddle point ξ limited to the second derivative, $g(z) = g(\xi) + g'(\xi)(z-\xi) + (1/2)g''(\xi)(z-\xi)^2$, and taking into account $g'(\xi) = 0$, the parameter s is:

$$s = \sqrt{-\frac{1}{2}g''(\xi)}(z-\xi). \tag{3}$$

Denoting the beginning and the end of the contour C by s_1 and s_2 we have:

$$I(\lambda) = \sqrt{-2g''(\xi)}e^{i\lambda g_I(\xi)} \int_{s_2}^{s_1} e^{\lambda(g_R(\xi)-s^2)}G(s)\,\mathrm{d}s. \tag{4}$$

3. Performing integration. The integrand, especially for large positive λ values, is small everywhere except the vicinity of the saddle point ξ ($s = 0$). For a slowly varying function $G(s)$, assuming $G(s) \cong G(s=0) = G(\xi)$ and extending the interval into $(-\infty, +\infty)$, the Gauss integral of the type $\exp(-\lambda s^2)$ appears, what leads to the result:

$$I(\lambda) = \sqrt{\frac{-2\pi}{\lambda g''(\xi)}}e^{\lambda g(\xi)}G(\xi). \tag{5}$$

Equation (5) is often called the first order saddle point approximation. If the integrand strictly fulfils the above listed conditions, it can be easily evaluated. Unfortunately, in practice such a situation is rather rare. On the contrary, usually difficulties

arise, for example multi-valued functions, for which a construction of the Riemann surface with singularities, branch points and branch cuts is necessary. In acoustic problems, the double-valued function (containing square roots) often appears, the λ parameter is not large or $G(z)$ is not a slowly varying function near the saddle point.

For these reasons some improvements are introduced to the basic method, two of which, applied in the paper to solve the problems considered, will be concisely reminded.

2.1. Inclusion of the argument of the $G(z)$ function into the exponential function

This is the easiest way of improving the approximation and it is quite efficient in some cases [1, 7]. Expressing $G(z) = |G(z)| \exp[i\Gamma(z)]$, the function in the exponent takes the form:

$$g_1(z) = g(z) + (i/\lambda)\Gamma(z), \tag{6}$$

the saddle point criterion is:

$$g'(\xi) + (i/\lambda)\Gamma'(\xi) = 0, \tag{7}$$

and the integral (1) is as follows:

$$I(\lambda) = \sqrt{\frac{-2\pi}{\lambda g_1''(\xi)}} e^{\lambda g(\xi)} G(\xi). \tag{8}$$

In this approximation the phase of the function $G(z)$ affects the saddle point location and the steepest descent path. This variant of the method is especially suitable for functions of steady amplitude and a varying argument.

2.2. Second and further approximations

As mentioned before, the basic formula (5) is often called the first order approximation. To obtain the second approximation, the integrand $G(z)$ is expanded into the Taylor series in the neighbourhood of the saddle point, ξ. This is equivalent to expanding $G(s)$ in the neighbourhood of $s = 0$: $G(s) \cong G(0) + G'(0)s + (1/2)G''(0)s^2$ and leads to the formula [1–2]:

$$I(\lambda) = \sqrt{\frac{-2}{g''(\xi)}} e^{\lambda g(\xi)} \left(\sqrt{\frac{\pi}{\lambda}} G(\xi) - \frac{\pi G''(\xi)}{2\lambda g''(\xi)} \right). \tag{9}$$

The formulae derived in this section are valid under the assumption that in the saddle point, ξ, the second derivative $g''(\xi) \neq 0$, otherwise the integrals obtained become infinite. The case $g'(\xi) = 0$, $g''(\xi) = 0$ cannot be treated by means of this method.

3. Plane-wave representation of a spherical wave

The field is generated by a point source located in the upper half plane; the lower medium is of higher velocity (air/water, water/sand), what results in the phenomena of total reflection above the critical angle. One of the consequences is the appearance of a lateral wave well known in shallow water acoustics and seismology.

The first step is to present the plane wave integral representation of a spherical wave. Lets assume a point sound source of a monochromatic wave with the time dependence $\exp(-i\omega t)$. Thus the acoustic potential at a distance R from the source is $\Phi_0(R) = R^{-1}\exp(ikR)$, where $k = \omega/c$ is the wave number, ω the wave frequency and c the speed of sound. In Cartesian co-ordinates $(x,\, y,\, z)$, the potential of a spherical wave takes the form of a surface integral [1, 11]

$$\Phi_0(R) = \frac{e^{ikR}}{R} = \int_{-\infty}^{+\infty}\int_{-\infty}^{+\infty} \frac{1}{2\pi k_z} e^{i(k_x x + k_y y + k_z z)}\,\mathrm{d}k_x\,\mathrm{d}k_y, \qquad z \geq 0, \tag{10}$$

where $R^2 = x^2 + y^2 + z^2$ and $k^2 = k_x^2 + k_y^2 + k_z^2$. The integration is performed over the entire plane $(k_x,\, k_y)$ and allows for imaginary values of k_z.

The physical interpretation of the above expression is as follows: each point in the $(k_x,\, k_y)$ plane provides a contribution to the spherical wave $R^{-1}\exp(ikR)$ in the form of a plane wave. Points located inside the circle of radius k (real k_z) correspond to homogeneous waves, points outside the circle (imaginary k_z) represent inhomogeneous waves. Assuming, for physical reasons, the imaginary part of k_z positive

$$k_z = k\cos\theta = k\cos(\theta' + i\theta'') = k(\cos\theta'\cosh\theta'' - i\sin\theta'\sinh\theta''), \tag{11}$$

introducing spherical coordinates $k_x = k\sin\theta\cos\varphi$, $k_y = k\sin\theta\sin\varphi$, and polar co-ordinates $x = r\cos\varphi_1$, $y = r\sin\varphi_1$, and substituting [18]

$$\int_0^{2\pi} e^{i(k_x x + k_y y)}\mathrm{d}\varphi = 2\pi J_0(kr\sin\theta), \tag{12}$$

the potential of the spherical wave is expressed as a contour integral of a complex variable θ:

$$\Phi_0(R) = ik\int_0^{\pi/2 - i\infty} J_0(kr\sin\theta)e^{ikz\cos(\theta)}\sin\theta\,\mathrm{d}\theta, \tag{13}$$

where $r = R\sin\alpha$, $z = R\cos\alpha$, $J_0(w)$ denotes the Bessel function of order zero. As $k_z = k\cos\theta$, real k_z changing within the limits $0 \leq k_z \leq k$ corresponds to real values of θ changing from $\pi/2$ to 0. For imaginary k_z with an increasing positive imaginary part, the range of θ varies from $\pi/2$ to $\pi/2 - i\infty$.

Up to this point no approximations have been executed, so the last representation of a spherical wave (13) is an exact formula.

The acoustic potential of a spherical wave can be expressed also by means of the Hankel function $H_0^{(1)}(w)$ [18]. There are two main reasons to stick to that form: the symmetry properties of the new contour of integration and the simplicity of asymptotic form of the Hankel function. Applying the identity $J_0(w) = (1/2)[H_0^{(1)}(w) - H_0^{(2)}(w)]$ and substituting under the integral the Hankel's function the asymptotic form valid for $|w| \gg 1$:

$$H_0^{(1)}(w) = \sqrt{\frac{2}{\pi w}} e^{i(w-\pi/4)} \left(1 + \frac{1}{8iw} + ...\right) \cong \sqrt{\frac{2}{\pi w}} e^{i(w-\pi/4)}, \tag{14}$$

the spherical wave is decomposed into an infinite number of plane waves incident at the interface at an angle θ

$$\Phi_0(R) = \frac{e^{ikR}}{R} = c \int_{-\pi/2+i\infty}^{\pi/2-i\infty} e^{ikR\cos(\theta-\alpha)} \sqrt{\sin\theta}\, \mathrm{d}\theta, \tag{15}$$

where $c = [ik/(2\pi R \sin\alpha)]^{1/2}$.

Each of these contributing plane waves obeys the simple rules of reflection and transmission (Snell's law) and (15) has the form suitable for applying the saddle point method.

4. The fluid-fluid interface

In what follows, the reflection of a spherical wave at the fluid-fluid boundary [1–3, 7, 11] is considered.

The point source (Fig. 2) is located at the height z_s in a medium characterised by the density ρ_1 and the speed sound c_1 equal to ρ_2 and c_2 in the lower medium, respectively. We assume $c_2 > c_1$.

The plane wave reflection coefficient is [1]

$$V(\theta) = \frac{m\cos\theta - \sqrt{n^2 - \sin^2\theta}}{m\cos\theta + \sqrt{n^2 - \sin^2\theta}}, \tag{16}$$

where $m = \rho_2/\rho_1$ and $n = c_1/c_2$. For $n < 1$ the critical angle is defined as $\theta_{\mathrm{cr}} = \arcsin(n)$. As long as the media are homogeneous, n and θ_{cr} are real (the attenuation constant is represented by the imaginary part of the sound speed, which results in a complex n with a positive imaginary part). The potential of the reflected field is calculated

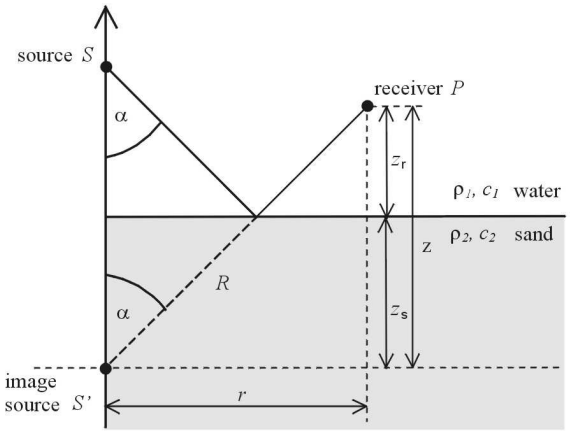

Fig. 2. Geometry of the reflected field. The boundary between the two media $(c_2 > c_1)$ is located at $z = 0$. The actual source S is substituted by the image source S' situated in the lower medium.

introducing the reflection coefficient under the integrand of Eq. (13):

$$\Phi_{\mathrm{ref}}(R,\alpha) = ik \int_0^{\pi/2-i\infty} J_0(kr\sin\theta) e^{ikz\cos\theta} V(\theta)\sin\theta\,\mathrm{d}\theta. \tag{17}$$

Equation (17) is the exact formula representing the potential of the reflected wave and can be useful for numerical calculations. However, because of the properties of the integrand and the infinite interval of integration, calculations with the proper accuracy assumed would involve time-consuming procedures and, which is even more important, would not provide a physical insight into the considered phenomena.

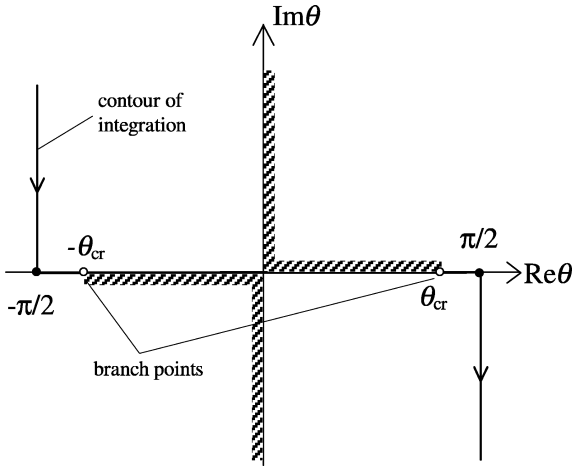

Fig. 3. Contour of integration for the reflected field (Eq. (18)) in the complex θ plane. The branch points $(\pm\theta_{\mathrm{cr}} = \arcsin(n))$ and branch cuts $(\pm\theta_{\mathrm{cr}} \pm i\infty)$ are also marked.

To solve the problem by means of the saddle point method, an approximate formula of the form corresponding to Eq. (15) will be applied:

$$\Phi_{\mathrm{ref}}(R,\alpha) = c \int\limits_{-\pi/2+i\infty}^{\pi/2-i\infty} e^{ikR\cos(\theta-\alpha)} V(\theta)\sqrt{\sin\theta}\,\mathrm{d}\theta. \tag{18}$$

Figure 3 presents the adequate contour of integration. Because of the asymptotic form of the Hankel function, Eq. (18) is valid only for $|kr\sin\theta| \gg 1$.

In Eq. (18), when compared with Eq. (1):

$$\lambda = kR, \qquad g(\theta) = i\cos(\theta-\alpha), \qquad G(\theta) = V(\theta)\sqrt{\sin\theta}, \tag{19}$$

and the saddle point occurs at $\xi = \alpha$, so it equals to the angle of incidence of the wave reaching the receiver.

Examining if the $V(\theta)$ function fulfils the required conditions, one notices that regarding angles of incidence $\theta < \theta_{\mathrm{cr}}$, $V(\theta)$ is real and for angles not very close to θ_{cr} it is varying slowly (cf. Figs. 4–5).

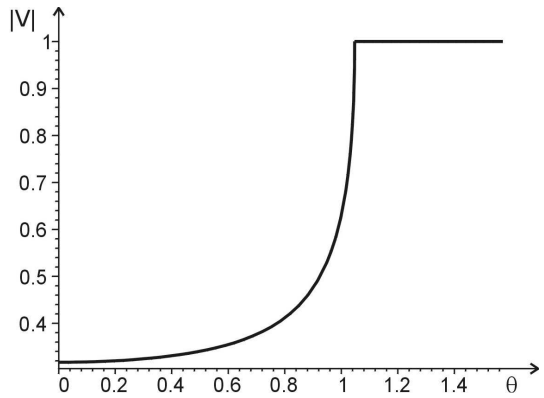

Fig. 4. Modulus of the reflection coefficient $V(\theta)$ on the water/sand boundary ($\theta_{\mathrm{cr}} = \pi/3$) and real θ. Apart from the vicinity of θ_{cr} it is varying slowly.

Some difficulties arise when drawing the steepest descend path. Because of the square root component, $V(\theta)$ is a two-valued function determined on the two-leaf Riemann space, each leaf for one value of the square root. Deforming the contour of integration into the steepest descend path one has to be aware when crossing singularities, branch points or branch cuts. The deformed contour of integration must begin and end on the same leaf of Riemann surface. The branch cuts of the integrand presented in Fig. 3 begin at branch points for which $n^2 - \sin^2\theta = 0$, which means that branch points are $\pm\theta_{\mathrm{cr}}$.

For $\alpha < \theta_{\mathrm{cr}}$, the branch line $(\theta_{\mathrm{cr}},\, i\infty)$ is crossed twice and the deformation rules are fulfilled as indicated in Fig. 6.

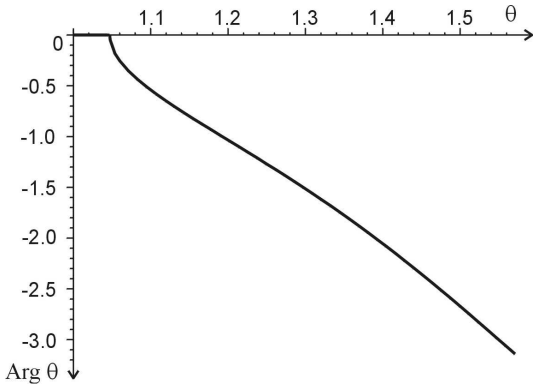

Fig. 5. Argument of the reflection coefficient $V(\theta)$ on the water/sand boundary ($\theta_{\rm cr} = \pi/3$) and real θ. For $\theta < \theta_{\rm cr}$ it is equal to 0.

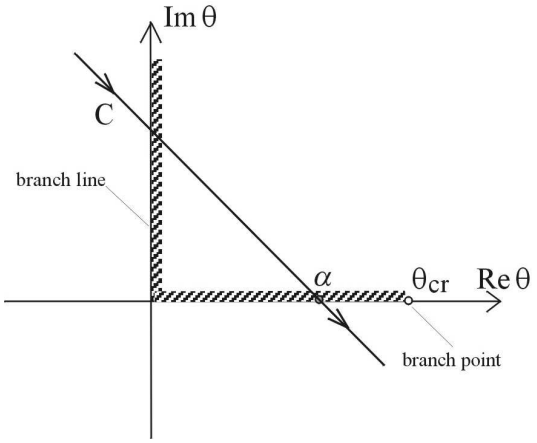

Fig. 6. Contour of integration for the reflected field in the complex θ plane for the angles of incidence $\theta < \theta_{\rm cr}$. The branch line is cut two times, the beginning and the end of the integration contour are located on the same leaf of the Riemann surface.

The result is, according to Eq. (18),

$$\Phi_{\rm ref}(R,\alpha) = \int\limits_{c} F(\theta)\,{\rm d}\theta = V(\alpha)\frac{e^{ikR}}{R}, \qquad \alpha < \theta_{\rm cr}, \tag{20}$$

where $F(\theta)$ denotes the integrand of Eq. (18).

The question arises if the last equation is fulfilled for larger angles of incidence although not very close to the critical angle: $\alpha > \theta_{\rm cr}$. Deformation of the integration contour C $[-\pi/2 + i\infty$ .. $\pi/2 - i\infty]$ into the steepest descend path, performed in the same way as before, would lead to a situation where the beginning and the end of the integration contour were situated on two different leafs of the Riemann surface. To avoid

this, the integration path has to be chosen such that the branch cut is passed round as shown in Fig. 7.

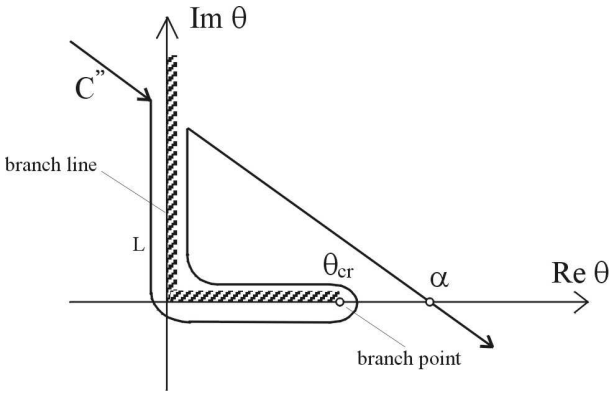

Fig. 7. Contour of integration for angles of incidence $\alpha > \theta_{\rm cr}$ after the properly executed deformation consists of curves C'' and L, the last one passing around the branch cut $(\theta_{\rm cr},\ i\infty)$.

Now, the potential of the reflected wave can be expressed symbolically in the form

$$\Phi_{\rm ref}(R,\alpha) = V(\alpha)\frac{e^{ikR}}{R} + \int\limits_L F(\theta)\,{\rm d}\theta, \tag{21}$$

where the second component represents the lateral wave.

Due to symmetry properties, the integral over L, expressing the lateral wave, can be written as

$$\begin{aligned}\Phi_{\rm lat}(R,\alpha) &= \int\limits_L F(\theta)\,{\rm d}\theta \\ &= c\int\limits_{\theta_{\rm cr}}^{i\infty} e^{ikR\cos(\theta-\alpha)}\,\frac{4m\cos\theta\sqrt{n^2-\sin^2\theta}}{(m\cos\theta)^2-(n^2-\sin^2\theta)}\sqrt{\sin\theta}\,{\rm d}\theta.\end{aligned} \tag{22}$$

It seems that the saddle point method fails in this case, as it does not account for the lateral wave arising according to Fermat's principle. However, a detailed analysis of the integrand in Eq. (18) leads to the conclusion that the argument of $V(\theta)$ is not varying slowly for $\theta > \theta_{\rm cr}$ (cf. Figs. 4–5 and Figs. 8–9) and therefore it does not satisfy the condition of applicability of the saddle point method in its basic version. The necessity arise to make use of Eqs. (6)–(8) and introduce the argument of the function $V(\theta)$ into the exponential function.

Denoting $V(\theta) = |V(\theta)|\exp[i\Gamma(\theta)]$, for angles greater than that of total internal reflection

$$|V(\theta)| = 1, \qquad \Gamma(\theta) = -2\tan^{-1}\frac{\sqrt{\sin^2\theta - n^2}}{m\cos\theta}, \qquad \theta > \theta_{\rm cr}, \tag{23}$$

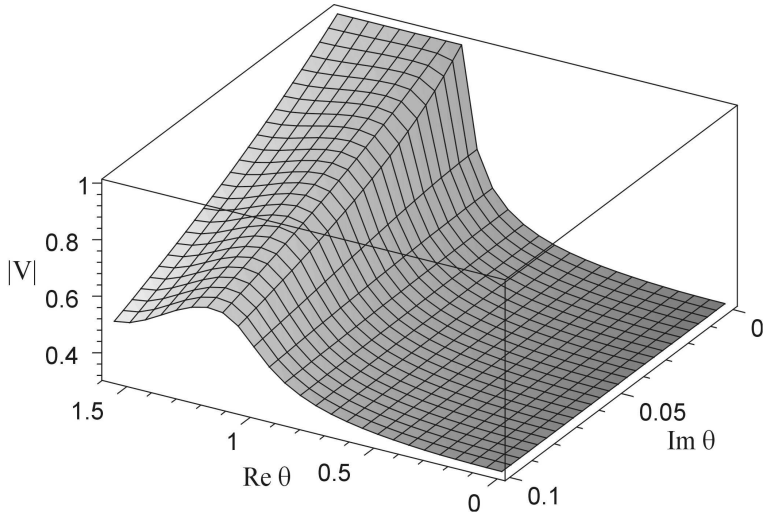

Fig. 8. Modulus of the reflection coefficient $V(\theta)$ for complex θ. For $\mathrm{Im}(\theta) = 0$ one should notice the curve presented in Fig. 4.

what leads to the following equation determining the saddle point:

$$g_1(\theta) = i\cos(\theta - \alpha) - \frac{2i}{kR}\tan^{-1}\frac{\sqrt{\sin^2\theta - n^2}}{m\cos\theta} = 0. \tag{24}$$

Equation (24), solved by means of numerical methods, has two roots corresponding to two saddle points. One of them is close to the incident angle ($\xi_1 < \alpha$), but a little less, the other one is very close to the critical angle point, but little above it ($\xi_2 \cong \theta_{\mathrm{cr}}$).

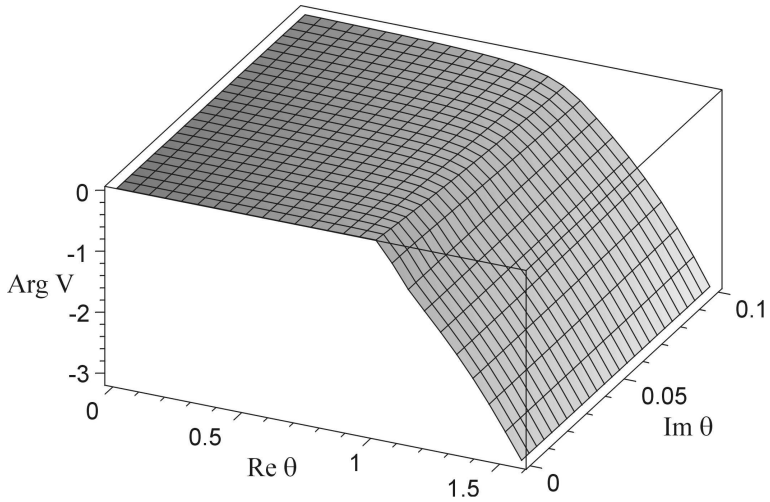

Fig. 9. Argument of the reflection coefficient for complex θ. One should notice that for real angles $\theta < \theta_{\mathrm{cr}}$ it equals 0 as shown in Fig. 5.

The presence of two saddle points can be seen in Fig. 10 by comparing the exponent of the basic and improved methods. Introduction of the argument of $V(\theta)$ into the exponential results in the occurrence of the second saddle point. This leads to the following expression for the potential of the lateral wave similar to Eq. (8):

$$\Phi_{\mathrm{lat}} = \sqrt{\frac{-2\pi i}{kRg_1''(\xi_2)}}\,, \tag{25}$$

where the function $g_1(\theta)$ is defined by Eq. (24). The potential of the lateral wave is not presented explicitly because of the complicated form of the second derivative of g_1. In addition, the method requires $g_1''(\xi) \neq 0$.

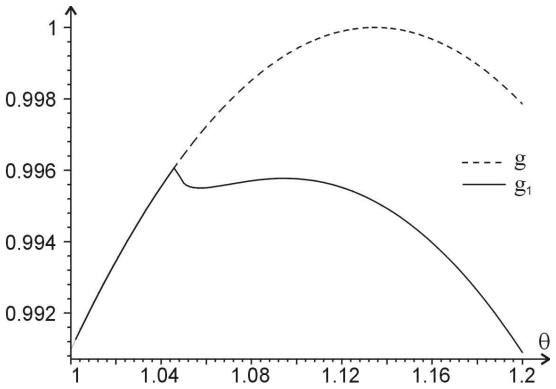

Fig. 10. The g and g_1 functions for the water/sand boundary, the angle of incidence α exceeding the critical angle θ_{cr} by 5° when the vertical distance between the image source and receiver, z is 10λ. One may notice two extremes (saddle points) of the g_1 connected with the lateral and Snell's waves.

For $\alpha < \theta_{\mathrm{cr}}$, the argument of $V(\theta)$ equals 0 ($\Gamma = 0$). Therefore there exists only one saddle point at $\xi = \alpha$. For $z = 10\lambda$, the real solution occurred starting from the angle of 64°, for $z = 20\lambda$ – from 63°, and for $z = 100\lambda$ – from 61°. For small distances z and angles close to the critical one, one should expect complex values of the saddle points. For real values of the angle, the function g_1 has one extreme (Fig. 11) and a point of inflection. In this region, the considered modification of the method fails.

The following table represents values of saddle points calculated for the water/sand boundary ($\theta_{\mathrm{cr}} = 60^\circ$, $n = 0.866$, $m = 1.67$) for different vertical distances between the image source and the receiver expressed in wavelengths ($z = 10\lambda$, 20λ, and 100λ). The calculations have been performed starting from $\alpha = 61^\circ$.

All in all, for angles of incidence $\alpha > \theta_{\mathrm{cr}}$, the potential of the reflected wave can be represented as a sum of two waves: the wave reflected according to the Snell's law and the lateral wave:

$$\Phi_{\mathrm{ref}} = \Phi_{\mathrm{Snell}} + \Phi_{\mathrm{lat}}, \qquad \alpha > \theta_{\mathrm{cr}}, \tag{26}$$

where $\Phi_{\mathrm{Snell}} = V(\xi_1)[\sin(\xi_1)/\sin(\alpha)]^{1/2} R^{-1}\exp(ikR)$ instead of $V(\alpha)R^{-1}\exp(ikR)$ as before. A geometrical representation of these waves is given in Fig. 12.

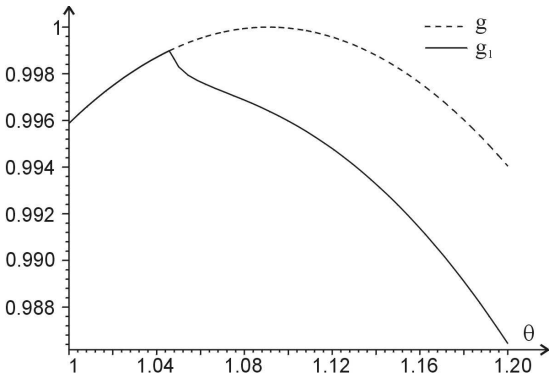

Fig. 11. The same as above (Fig. 10), but for the angle of incidence α exceeding the critical angle $\theta_{\rm cr}$ by 2.5°. The g_1 function has one extreme and one point of deflection. In the vicinity of the critical angle $\theta_{\rm cr}$ the method fails since the saddle points become complex (cf. Table 1a).

Table 1. Values of saddle points ξ_1, ξ_2, versus angle of incidence α calculated for the water/sand boundary ($\theta_{\rm cr} = 60^\circ$, $n = 0.866$, $m = 1.67$) for different vertical distances image source – receiver: a) $z = 10\lambda$, b) $z = 20\lambda$, and c) $z = 100\lambda$.

a)

α	61	62	63	64	65	66	67	68	69	70	75	80	85
ξ_1	#	#	#	#	62.71	64.06	65.25	66.37	67.47	68.55	73.83	79.11	84.49
ξ_2	#	#	#	#	60.57	60.31	60.20	60.14	60.10	60.07	60.02	60∗	60∗

b)

α	61	62	63	64	65	66	67	68	69	70	75	80	85
ξ_1	#	#	61.41	62.83	63.99	65.08	66.15	67.20	68.24	69.27	74.41	79.55	84.75
ξ_2	#	#	60.53	60.20	60.11	60.07	60.05	60.03	60.02	60.01	60∗	60∗	60∗

c)

α	61	62	63	64	65	66	67	68	69	70	75	80	85
ξ_1	60.39	61.70	62.76	63.79	64.81	65.82	66.83	67.84	68.84	69.85	74.88	79.91	84.95
ξ_2	60.39	60.03	60.01	60∗	60∗	60∗	60∗	60∗	60∗	60∗	60∗	60∗	60∗

– no real solutions,
∗ – values differ from 60° by less than 0.01°.

For $\alpha \to \theta_{\rm cr}$, both the rays merge, the saddle points ξ_1 and ξ_2 are equal to each other and in this case the modification of the saddle point method presented here fails because in the vicinity of $\theta_{\rm cr}$, called the caustic region, the function $V(\theta)$ must not be treated as a slowly varying function (Figs. 4, 5). This case requires further modification of the saddle point method.

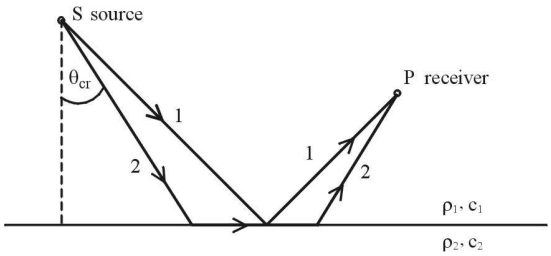

Fig. 12. Schematic representation of the Snell's (1) and lateral (2) reflected waves on a plane boundary between two homogenous media for the reflection coefficient $n < 1$.

5. The far field of a circular duct

The problem of the acoustic field inside and outside a semi-infinite circular waveguide was discussed in detail in the papers [14–16] published by the authors. Herein only benefits resulting from the application of the saddle point method are presented and similarities in the approach to both the problems are underlined.

Considering harmonic vibrations, the l-th mode acoustical potential of a semi-infinite cylindrical duct of radius a, with the outlet at $z = 0$, takes in cylindrical coordinates the form [6, 14]:

$$\begin{aligned}\Phi_l(\rho, z) &= \frac{J_0(\mu_l \rho/a)}{J_0(\mu_l)} e^{-i\gamma_l z} \\ &\quad + \frac{1}{4} ia \int_{-\infty}^{\infty} e^{iwz} v F_l(w) \left\{ \begin{array}{l} H_0^{(1)}(v\rho) J_1(va), \ \rho > a \\ H_0^{(1)}(v\rho) J_1(va), \ \rho < a \end{array} \right\} \mathrm{d}w, \end{aligned} \tag{27}$$

where w and v are the axial and radial wavenumbers, respectively, $w^2 + v^2 = k^2$, $F_l(w)$ is the Fourier transform of the discontinuity (jump) of the potential on the duct's wall. The first term in Eq. (27) represents the incident wave, the so-called l-th Bessel mode, the integral represents the field excited due to reflection and diffraction phenomena [6, 14]. Inside the duct it takes the form of superposition of Bessel modes [6, 14], outside the duct, in the far field, it can be evaluated by means of the saddle point method [14].

Expressing the axial wavenumber w by means of he complex variable θ, $w = k \sin\theta$, and applying the asymptotic form of the Hankel function (Eq. (14)), the following formulae result:

$$\Phi_l(R, \alpha) = c e^{i\pi/4} \int_{C_1} W_l(\theta) e^{ikR\sin(\alpha-\theta)} \sqrt{\cos\theta}\, \mathrm{d}\theta, \tag{28}$$

$$W_l(\theta) = J_1(ka\cos\theta) F_l(k\sin\theta) \cos\theta \left(1 + \frac{1}{8ikR\sin\alpha\cos\theta}\right), \tag{29}$$

$c = (ia/4)\sqrt{2k/(\pi R \sin\alpha)}$. The contour C_1 starts at $\pi/2 - i\infty$, passes near $\pi/2$, along the real axis to the $-\pi/2$ and asymptotically to $-\pi/2 + i\infty$. One may notice

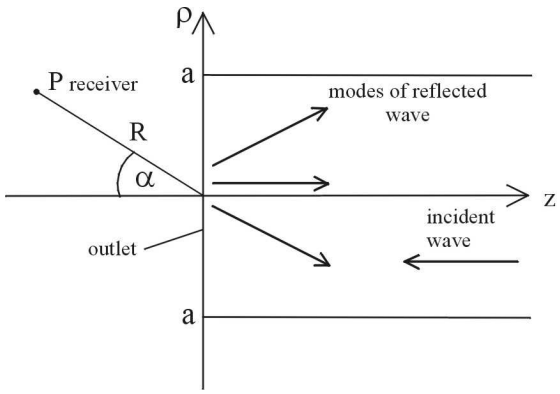

Fig. 13. Geometry of the cylindrical wave-guide of radius a radiating outside due to reflection and diffraction phenomena at the outlet at $z = 0$. The location of receiver P is described by $(R,\ \alpha)$.

the correspondence between this contour and that presented in Fig. 3, however now the branch points are located at $\pm\pi/2$. From a comparison of Eqs. (28), (1) and (19), it comes out that λ and $g(\theta)$ are the same, but $G(\theta) = W_l(\theta)\sqrt{\cos\theta}$.

Following the rules of the method, the result obtained is:

$$\Phi_l(R,\alpha) = d_l(\alpha)\frac{e^{ikR}}{R}\,, \tag{30}$$

where the directivity coefficient $d_l(\alpha)$ takes the form [14]:

$$d_l(\alpha) = \frac{1}{2}ka\sin\alpha J_1(ka\sin\alpha)F_l(-k\cos\alpha), \tag{31}$$

In the first approximation, the potential has the form of a spherical wave multiplied by the directivity function.

Many acoustic problems require the application of more precise formulae for the potential, thus the need to develop the second and further approximations arises. To obtain the second approximation, the integrand has to be expanded into a series in the neighbourhood of the saddle point [16]. Limiting the expansion to the terms containing the second power of s at the most, the results are:

$$\Phi_l(R,\alpha) \;=\; D_l(R,\alpha)\frac{e^{ikR}}{R}\,, \tag{32}$$

$$\begin{aligned} D_l(R,\alpha) \;=\; & d_l(\alpha) + \frac{ia}{2R}\Bigg[-\frac{d_l(\alpha)}{8\sin^2\alpha} \\ & + \cos\alpha\frac{d}{d\cos\alpha}(d_l(\alpha)) - \frac{\sin^2\alpha}{2}\frac{d^2}{d\cos^2\alpha}(d_l(\alpha))\Bigg]. \end{aligned} \tag{33}$$

Some numerical results of the directivity coefficient calculated according to Eqs. (30) and (32) are presented in Fig. 14.

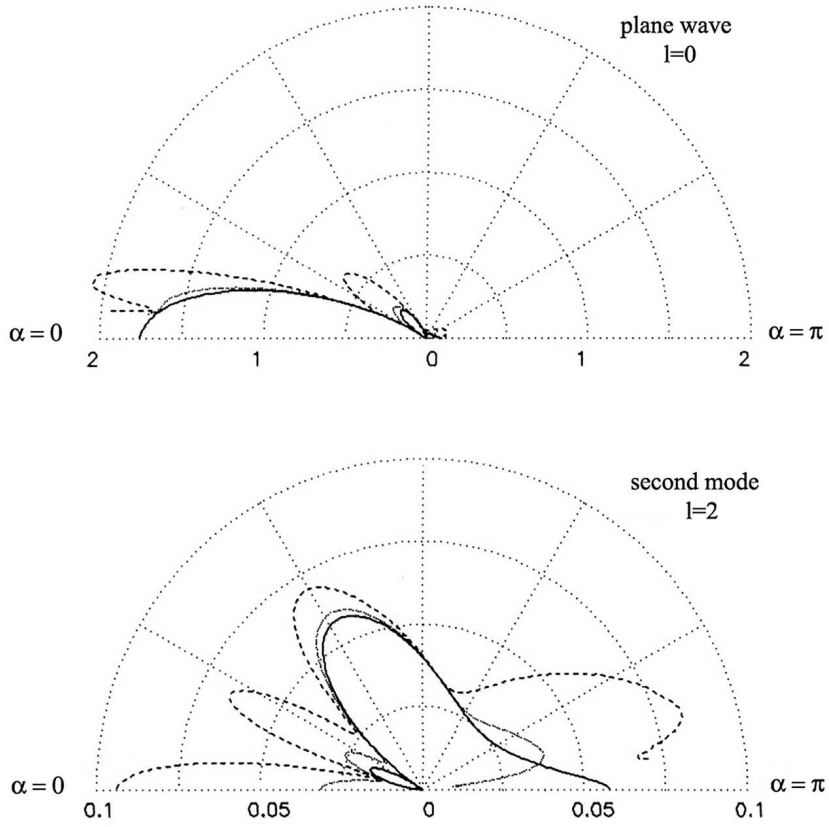

Fig. 14. Directivity coefficient for the far field radiated from a semi-infinite wave-guide; diffraction parameter $ka = 7.04$, allowing for propagation of the plane wave, and two Bessel modes along the duct. The first order approximation $kR \to \infty$ (continuous line), the second order approximation $kR = 7$ (dashed line) and $kR = 21$ (dotted line).

The second term in Eq. (33) describes the second order correction proportional to $1/R$, thus its contribution to the field potential decreases as the distance from the source increases. That is why Eq. (28) is often called the infinite distance approximations, $kR \to \infty$.

The possible improvement of the results obtained are computations of the field according to exact formula or further modification of the saddle point method resulting in complex saddle points.

6. Conclusions

The paper presents advantages resulting from the application of the approximate saddle point method to solve some general problems in acoustics. Two phenomena served as examples: the reflection of the spherical wave at a plane boundary between

two media (allowing for the lateral wave excitation) and the radiation from the outlet of a circular duct. The first problem is one of the main topics in hydroacoustics, the second one is vital in controlling the noise radiated from ducts, as, for example, the heating or ventilation systems. In both problems the acoustical potential has been chosen as a quantity describing the field. Although the derived exact integral formulae for the potential allow for numerical computations, the saddle point method provides new attractive features of the solution. First of all, it gives more physical insight into the considered phenomena.

In the wave reflection problem, it allows for a simple explanation of the occurrence of the lateral wave. If the angle of incidence is greater than the critical one, a second saddle point appears, which is "the mathematical manifestation" of the appearance of the lateral wave. Each term in the potential formula (Snell's wave and lateral wave) is associated with an adequate saddle point. This is even more spectaculare if the considered problem is more complicated, like in case of more than two-layers environments [20], when due to diffraction, apart from the straight coming wave also once, twice *etc*. reflected waves and the lateral wave appear. In the saddle point method approach, each of these waves is associated with a respective saddle point and the integral formula takes form of a sum of integrals attributed to different kinds of waves, which evidently simplifies not only the physical interpretation, but also the evaluation of each wave contribution to the sound field at the observation point.

In the circular duct problem, the application of the method results in the presentation of the far field outside inthe form of a spherical wave modified by the directivity coefficient. The coefficient, as presented in the paper, can be calculated with an assumed accuracy depending on which variant of the method is applied. The choice of the suitable variant is always based on a thorough examination of the mathematical properties of the functions and equations involved.

It may be interesting to consider what constitutes the background of these attractive features of the method. The answer may be in the relation between mathematics and physics.

Among the mathematical theories PENROSE [19] selected the "ideal/perfect" theories and expressed the opinion that an ideal theory is not only a useful tool to describe physical phenomena, but the deep inside of its structure contains the description of nature. This is why it is so efficient in describing physical world. The theory of analytic functions is, according to Penrose, an "ideal" theory. In the process of solving problems by means of the saddle point method a complex variable is introduced, the functions become analytic and the analytic function theory can be widely applied. This may be the source of the visible physical insight which, at least in the approximate method, carries on.

Even if the lateral wave were not discovered previously, the appearance of the second saddle point above the critical angle would indicate, that "there must be something" apart from the Snell's wave. In that way the mathematical theory reveals, by means of its equations, new physical phenomena.

To recapitulate, the main feature of the saddle point method is that it allows for a simple physical interpretation of the results obtained and gives more physical insight into the phenomena presented.

References

[1] BREKHOVSKIKH L. M., *Waves in layered media*, Academic Press, New York 1980.

[2] BREKHOVSKIKH L. M., *The reflection and refraction of spherical waves*, Uspiekhi Fiz. Nauk, **32**, 1, 1–42 (1949).

[3] BREKHOVSKIKH L. M., *The reflection of spherical waves at a plane interface between two media*, Journal of Technical Physics, **18**, 4, 455–482 (1948).

[4] WEIL H., *Ausbreitung elektromagnetischer Wellen uber einemebenen Leiter*, Ann. Physik, **60**, 481 (1919).

[5] SOMMERFELD A., *Uber die Ausbreitung der Wellen in der drahtlosen Telegraphie*, Ann. Physik, **28**, 665–736 (1909).

[6] WAJNSHTEJN L. A., *The theory of diffraction and the factorization method. Generalized Wiener–Hopf technique*, Golem Press, New York 1969.

[7] PLUMPTON N. G., TIND1E C. T., *Saddle point analysis of the reflected acoustic field*, J. Acoust. Soc. Am., **85**, 1115–1123 (1989).

[8] SARACCO G., CORSAIN G., LEANDRE J., GAZANHES C., *Propagation d'ondes spheriques monochromatiques a travers une interface plane fluide/fluide: applications numeriques et experimentales au dioptre plan air/eau*, Acustica, **73**, 21–32 (1991).

[9] SNAKOWSKA A., WITKOWSKI P., IDCZAK H., *The saddle point method applied to some problems in acoustics*, pp. 321–326, Proceedings of International Symposium on Hydroacoustics and Ultrasonics – EAA Symposium, Jurata 1997.

[10] SNAKOWSKA A., IDCZAK H., *The image of acoustical phenomena in mathematical equations – some examples* (in Polish), pp. 555–562, Proceedings of XLIX Open Seminar on Acoustics, Stare Jabłonki 2002.

[11] WESTWOOD E. K., *Complex ray methods for acoustic interaction at a fluid-fluid interface*, J. Acoust. Soc. Am., **85**, 5, 1872–1884 (1989).

[12] THOMASSON S. I., *Reflection of waves from a point source by an impedance boundary*, J. Acoust. Soc. Am., **59**, 4, 780–785 (1976).

[13] ENFLO B. O., ENFLO P. H., *Sound wave propagation from a point source over a homogenous surface and over a surface with an impedance discontinuity*, J. Acoust. Soc. Am., **82**, 6, 2123–2134 (1987).

[14] SNAKOWSKA A., *The acoustic far field of an arbitrary Bessel mode radiating from a semi-infinite unflanged cylindrical wave-guide*, Acustica, **77**, 53–62 (1992).

[15] SNAKOWSKA A., IDCZAK H., BOGUSZ B., *Modal analysis of the acoustic field radiated from an unflanged cylindrical duct – theory and measurement*, Acustica, **82** (1996).

[16] SNAKOWSKA A., *The energy distribution in the far field radiated from the semi-infinite unflanged cylindrical waveguide*, Archives of Acoustics, **17**, 4, 525–542 (1992).

[17] MORSE P., FESHBACH H., *Methods of theoretical physics*, Mc. Graw–Hill, London 1953.

[18] WATSON G. N., *A treatise on the theory of Bessel functions*, Cambridge University Press, Cambridge 1958.

[19] PENROSE R., *The Emperors New Mind*, Oxford University Press, 1997.

[20] LI L. W., LEE C. K., YEO T. S., *Wave mode and path characteristics in a four-layered anisotropic forest environment*, IEEE Trans. Antennas Propagat., **52**, 9, 2445–2455 (2004).